

Microstructure and Corrosion Behavior of Micro-Arc Oxidation Film on Magnesium Alloy

Li-lai Liu^{1,2}, Pei-xia Yang^{2,*}, Cai-na Su³, Hong-fei Guo², Mao-zhong An²

¹ Engineering Research Academy of Graphite New Materials, Heilongjiang Institute of Science and Technology, Harbin 150027, China

² School of Chemical Engineering and Technology, Harbin Institute of Technology, Harbin 150001, China

³ School of Applied Chemistry and Environmental Engineering, Xinyang Vocational and Technical College, Xinyang 464000, China

*E-mail: yangpeixia@hit.edu.cn

Received: 1 March 2013 / Accepted: 10 April 2013 / Published: 1 May 2013

The microstructure, composition and elemental depth profile of micro-arc oxidation film was analyzed by means of Scanning Electron Microscope (SEM), X-ray diffraction (XRD) and Energy Disperse Spectroscopy (EDS). The film is composed of an outer loose layer and an inner dense layer, a few circular pores present on the film surface, but merely in the outer loose layer, do not traverse through the inner dense layer to the metal substrate. The film is composed of forsterite phase Mg_2SiO_4 and magnesia MgO . The elemental depth profile shows that Mg, Si and O have a gradient distribution within the film. The gradient distribution of Mg, Si, O also indicated that the relative content of Mg_2SiO_4 decreased, while MgO increases in the depth direction to the alloy substrate. Combined with the impedance spectra collected after different exposure time to 3.5 % NaCl solution, a four-stage corrosion process was proposed to describe the corrosion behavior of micro-arc oxidation film on magnesium alloy.

Keywords: Magnesium alloy; Micro-arc oxidation; Structure; Corrosion; EIS

1. INTRODUCTION

Magnesium alloys have a number of applications in fields of automobile industry, aerospace components, communications and computer parts, etc. [1,2], due to their excellent physical and mechanical properties, such as low density, high specific strength, good welding ability, excellent damping capacity and good electromagnetic shielding characteristics [3,4]. However, magnesium alloys are highly susceptible to corrosion, which greatly restricts their widespread application,

especially in acidic environments and in salt-water conditions [5]. To enhance the corrosion resistance, several surface treatments such as chemical conversion coatings [6,7], anodizing [8], electroplating and electroless plating [9,10] have been researched. However, they are not adequate for use in some harsh service circumstances without further sealing.

Recently, a novel promising surface treatment method, micro-arc oxidation (MAO) [11], which is capable of protecting the valve metals and their alloys from both corrosion and wear, has been developed and applied to magnesium and its alloys [12-15]. However, the corrosion resistance provided by this method is not satisfaction in practical application. Severe pitting corrosion still occurs after long time immersion in 3.5 % NaCl solution [16]. For guiding researchers to exploit a more valuable craft to prevent the metal from pitting corrosion and to accelerate the practical application of PEO technology, it is essential to provide a detailed explanation on the corrosion mechanism of micro-arc oxidation film on magnesium alloy. The purpose of the present paper is to interpret the corrosion behavior using the impedance spectroscopy and correlate the corrosion mechanism with composition and microstructure of micro-arc oxidation film.

2. EXPERIMENTAL

The die-cast AZ31B magnesium alloy were used as the substrate material in the present study, its chemical composition(wt.%) was Al 2.5-3.5, Zn 0.6-1.4, Mn 0.2-0.1, Si \leq 0.1, Fe \leq 0.005, Cu \leq 0.05, Ni \leq 0.005, and Mg balance. PEO treatment device consisted of a high power supply unit, a stainless steel container that also served as the counter electrode, a stirring and cooling system, the specimens were served as the anode. Prior to PEO, the specimens were polished with alumina waterproof abrasive paper, degreased with acetone, followed by rinsing with distilled water, then anodized in solutions containing 6 g/L Na₂SiO₃, 2 g/L NaF, 2 g/L KOH and 10 ml/L glycerol at 30 mA/cm² for 15 min.

Scanning electron microscope (SEM, Hitachi S-4700) was used to observe the surface and cross-section morphology of micro-arc oxidation anodic film on magnesium alloy and energy disperse spectroscopy (EDS) attached to SEM was used to detect the elemental depth profile of micro-arc oxidation film. The phase composition of micro-arc oxidation film was analyzed by means of X-ray diffraction (XRD, Philips X'Pert, Holland) using a Cu K α radiation as the excitation source at a grazing angle of 5°. The EIS measurements were performed using an EG&G potentiostat (Model 273) in a 300 ml submarine type cell using a typical three electrode system, in which the counter electrode was platinum and a saturated calomel electrode (SCE) was used as reference. The working electrode was embedded with epoxy resin to leave 1 cm² metal surface contacting with 3.5 % NaCl solution made with A.R. chemicals and distilled water at 20 °C. When the corrosion potential remained stable, a sinusoidal ac perturbation of 10 mV amplitude around the open circuit potential (OCP) was then applied to the electrode over the frequency ranges 10 kHz ~ 0.01 Hz. The impedance spectra were collected as a function of exposure time up to 120 h of immersion.

3. RESULTS AND DISCUSSION

3.1 Surface and cross-sectional morphology

Fig. 1 shows surface and cross-sectional SEM micrographs of micro-arc oxidation film on magnesium alloy.

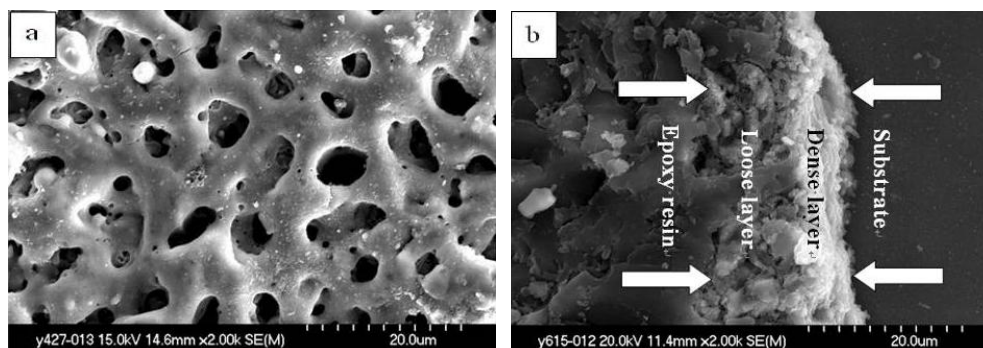


Figure 1. Surface (a) and cross-sectional (b) SEM micrographs of micro-arc oxidation film on magnesium alloy

Fig.1a shows quite a number of circular pores are seen to be present on the coating surface. The non-uniform growing pattern of the coating and trapping of oxygen bubbles in the coating growth process may be responsible for the extensive porosity of the film [17]. As shown in Fig.1b, the film is composed of two layers, an outer loose layer and an inner dense layer. The pores with diameters of 1~3 μm are seen to be present merely in the outer loose layer and to be somewhat interconnected; but do not traverse through the inner dense layer to the substrate. The loose layer corresponds to the porous structure as show in surface morphology of micro-arc oxidation film with large grains and loose porous structure.

3.2 Phase analysis

Fig. 2 shows the X-ray diffraction pattern of micro-arc oxidation film on magnesium alloy.

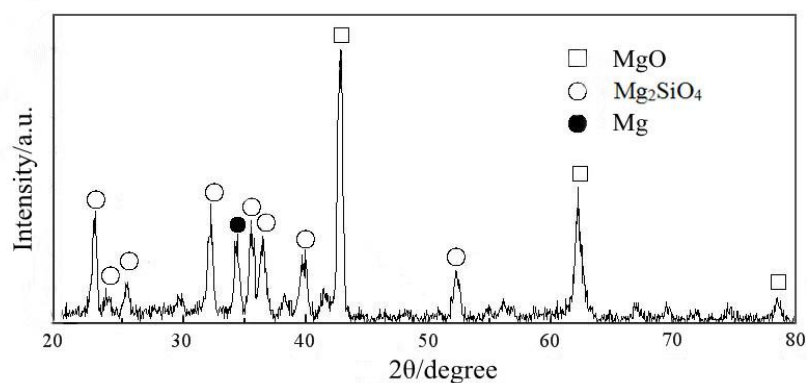
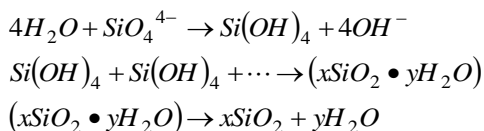


Figure 2. X-ray diffraction pattern of micro-arc oxidation film on magnesium alloy

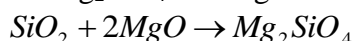
According to the XRD pattern, compared with ASTM cards, it can be concluded that the ceramic coating is mainly composed of forsterite phase Mg_2SiO_4 and magnesia MgO . Formation mechanism of MgO is similar to that of conventional anodization technology, i.e. simultaneously formation at the film/electrolyte and substrate/film interface by outward migration of Mg^{2+} from the substrate to the film/electrolyte interface and inward migration of O^{2-} from the electrolyte to the substrate/film interface [18]. The presence of Mg_2SiO_4 indicates that anion SiO_4^{4-} has incorporated into the film intensively. In aqueous solution, the sodium silicate is easy to be hydrolyzed to present in the form of $Si(OH)_4$. Simultaneously, due to the large amount heat resulting from discharge phenomenon, then was dehydrated to SiO_2 through a series of reactions [16].



Another possible path for the formation of SiO_2 is direct oxidation of SiO_4^{4-} under high electric field and high temperature conditions through the reaction [19].



Owing to the effect of high temperature in MAO process, both SiO_2 and MgO present in the fused state instantly. When micro arcs go out, under the cooling effect of electrolyte, a high temperature phase transformation occurs between SiO_2 and an excess of MgO , finally transforms into a mixture of Mg_2SiO_4 and MgO .



3.3 The elemental depth profile

The elemental distribution through the coating thickness is shown in Fig. 3.

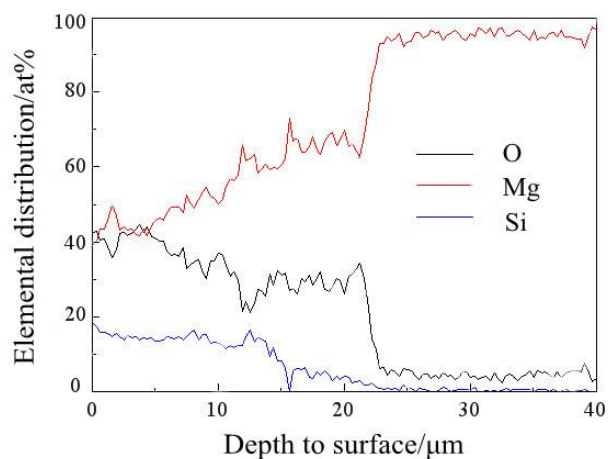


Figure 3. The elemental depth profile of micro-arc oxidation film on magnesium alloy

The content of Mg within the coating is lower than that in the alloy substrate, it gradually increased, in reverse, contents of O and Si gradually decreased. The presence of Si and O indicated

that the electrolyte components had intensively participated in the reactions of the coating formation. It should be noted that there was a peak, corresponding to each elemental linear distribution, indicated that the coating was composed of two layers, which is consistent with the SEM results of the coating cross-sectional morphology. The position of the peak was very close to the outer loose layer/inner dense layer interface derived from the SEM analysis. It may be attributed to pulling stress resulting from the shrinking effect of epoxy resin in solidification process or mechanical stress in polishing process, which resulted in a gap between the outer loose layer/inner dense layer interface, thus the elemental linear distribution exhibited a peak [20]. The gradient distribution of Mg, Si, O also indicated that the relative content of Mg_2SiO_4 decreased, while MgO increases in the depth direction to the alloy substrate.

3.4 Electrochemical impedance spectroscopy

EIS spectra collected from micro-arc oxidation film on magnesium alloy in Fig. 4.

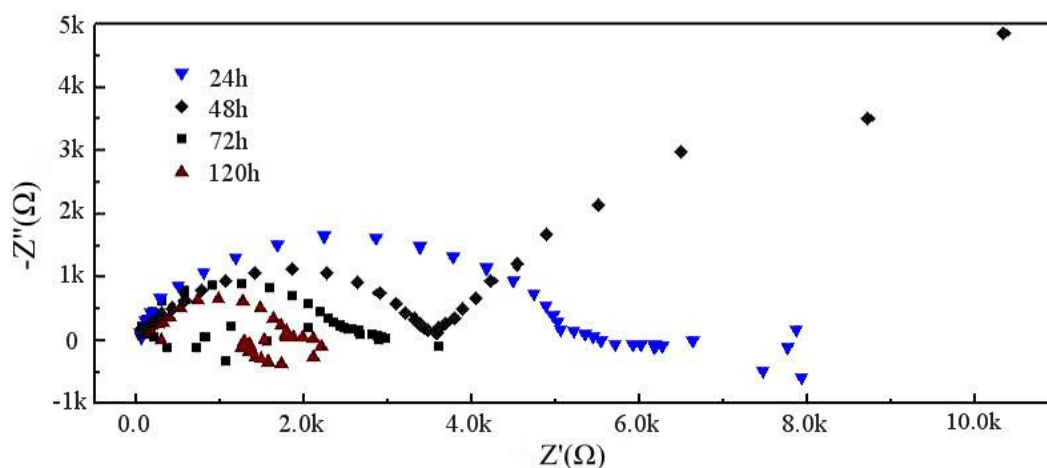


Figure 4. Nyquist plots of micro-arc oxidation film on magnesium alloy exposure to 3.5 % NaCl solution for different time

As shown in Fig. 4, the impedance data obtained for 24h of immersion shows a typical capacitive response at high frequencies and many unorderly points at low frequencies [21]. For 48 h of immersion in 3.5% NaCl solution, two capacitive responses are observable in Nyquist plots at high and low frequencies respectively. Upon immersion for 72 h, the impedance data again shows a capacitive response at high frequencies and many unorderly points at low frequencies. After immersion in NaCl solution over 120 h, except for a typical capacitive response at high frequencies, a low frequencies inductive loop, indicative of pitting corrosion, is seen apparently in the impedance data, and some unorderly points at medium frequencies could be seen. In addition, as immersion time increases the decrease of diameter with exposure time indicates that the response becomes less capacitive. The value of (R_1+R_2) should decrease with immersion time, however, Nyquist plots show that the value of

(R_1+R_2) at 48h is evidently larger than that at 24h. Moreover, the corrosion resistance is higher than that of 24h.

As shown in SEM micrograph of micro-arc oxidation film a few circular pores are seen to be present on the coating surface. The film is composed of two layers, an outer loose layer and an inner dense layer. The dense layer and loose layer exhibit different behavior in the corrosion process respectively. When no apparent destroy and apparent pitting corrosion occurred on the coating surface, the equivalent circuit was shown in Fig.5.

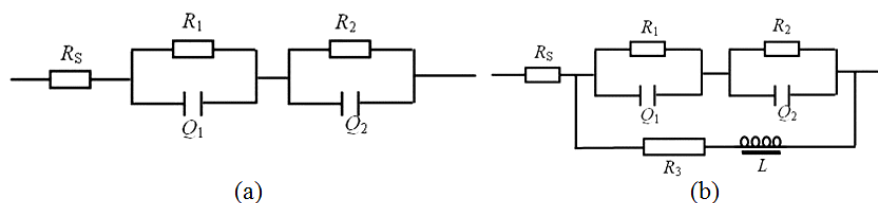


Figure 5. Equivalent circuit for corrosion process of micro-arc oxidation film immersion for 24、48、72 h (a) and for 120 h (b) in 3.5% NaCl solution (R_S —solution resistance; Q_1 、 Q_2 —constant phase elements corresponding to dense layer and loose layer; R_1 、 R_2 —dense layer and loose layer transfer resistance; R_3 —electrochemical reaction resistance; L —inductance)

The fitting results were illustrated in Fig. 6 and Table 1. The bad points were ignored in the fitting process because of the complexity of corrosion behavior of magnesium alloy.

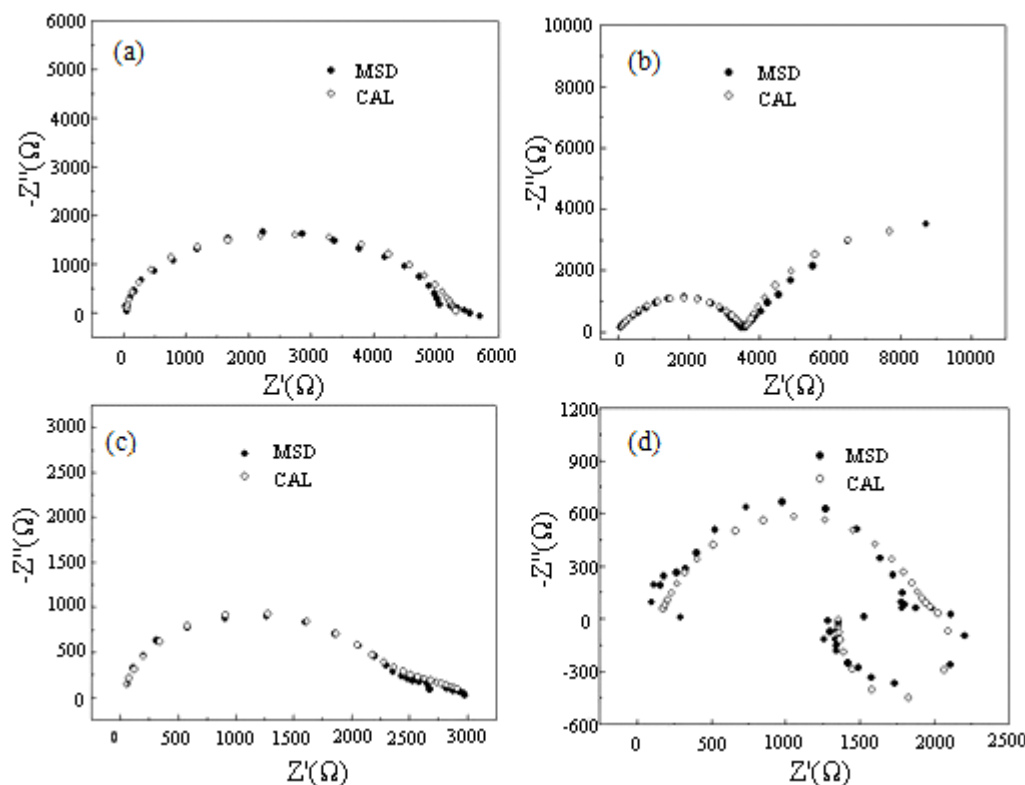


Figure 6. Fitting results of EIS plot of micro-arc oxidation film after immersion in 3.5% NaCl solution for 24 h (a); for 48 h (b); for 72 h (c) and for 120 h (d)

Table 1. Electrochemical parameters derived from the EIS plots

$R_1(\Omega)$	$R_2(\Omega)$	$R_3(\Omega)$	$Q_1(F\cdot cm^{-2})$	$Q_2(F\cdot cm^{-2})$	$L(F\cdot cm^{-2})$	n_1	n_2
3500	1656	---	2.13×10^{-7}	1.992×10^{-8}	---	0.8833	1
9299	3614	---	6.216×10^{-7}	7.774×10^{-4}	---	0.6927	0.7864
2112	839	---	4.48×10^{-8}	7.524×10^{-5}	---	0.8974	0.5723
1971	162.3	1355	8.394×10^{-7}	3.523×10^{-5}	143.7	0.7236	1

3.5 corrosion behavior of micro-arc oxidation film

According to the change of the Nyquist plots and corrosion behavior with immersion time in 3.5 % NaCl solution, combined with the composition and microstructure of micro-arc oxidation film on magnesium alloy, the corrosion process can be separated into four stages:

(1) It is suggested that water and electrolyte penetrate through the larger pores in the outer loose layer to reach the inner dense layer/outer loose layer interface, while do not penetrate through the dense layer to reach the coating/substrate interface at short immersion time because of the protective property of the inner dense layer, slight conversion of MgO to Mg(OH)₂ also occurs at the surface inside the pores and a little corrosion product is adsorbed on the film, which contributes to the unorderly points at low frequency [22].

(2) With the penetration of solution into the porous layer and slow thinning of the MgO dense layer, the corrosion resistance decreases and corrosion products increase gradually. After immersion in NaCl solution over 48 h, blocking of pores occurs within the outer porous layer owing to the volume expansion effect, resulting from the conversion of MgO to Mg(OH)₂. In this period, the penetration of solution was blocked, both the inner dense layer and the outer porous layer have a protective effect, corresponding to the two capacitive loops at high and low frequency respectively. The corrosion resistance is higher than that of 24 h in short period indicating that decreasing of porosity in porous layer is benefit to improve the corrosion resistance.

(3) With increasing of corrosion products and volume expansion, owing to the mechanical stress, the pores were finally broken down. At the same time, more corrosion products were adsorbed on the coating surface, corresponding to the unorderly points at low frequency, thus, the form of Nyquist plot in this period is similar to that of 24 h immersion.

(4) With increasing of immersion time (over 120 h), not only the outer porous layer but also the partial inner dense layer was also penetrated by Cl⁻, so corrosion of alloys substrate occurs. In this period, some partial film has a protective property, corresponding to the capacitive loop at high frequency, and in some partial areas, pitting corrosion of Mg alloy occurs independently, corresponding to the inductive loop at low frequency.

Once long time immersion is employed in 3.5 % NaCl solution, finally, it is suggested that a large amount of MgO is converted to lower density Mg(OH)₂ in the pores, resulting in the slow thinning of the MgO dense layer and volume expansion, which in turn causes further cracking of the micro-arc oxidation film. The cracks provide another pathway for penetration of NaCl solution and accelerate the hydration of MgO within the coating. A white precipitate, Mg(OH)₂, was seen to form at

the pits and to fall into solution, depositing on the base of the cell, and the alloy surface became porous and gray in color.

4. CONCLUSIONS

The ceramic coating was composed of outer porous layer and inner dense layer. The pores were seen to present merely in the outer loose layer. The ceramic coating was mainly composed of forsterite phase Mg_2SiO_4 and MgO . The content of Mg through the coating thickness gradually increased, in reverse, contents of O and Si gradually decreased from the coating surface to the alloy substrate. A four-stage corrosion process was proposed to describe the corrosion behavior of micro-arc oxidation film on magnesium alloy: Penetrating through the outer loose layer to reach the inner dense layer/outer loose layer interface; slow thinning of inner dense layer and blocking of pores; broken down of outer loose layer because of volume expansion; and pitting corrosion of metal substrate.

ACKNOWLEDGEMENTS

The work is supported by Young talents program funding of Heilongjiang institute of science and technology.

References

1. D. Eliezer, E. Aghion, F. H. Fries, *Adv. Perform. Mater.*, 201 (1998) 201.
2. H. Friedrich, S. Schumann, *J. Mater. Process. Tech.*, 117 (2001) 276.
3. B. L. Mordike, T. Ebert, *Mater. Sci. Eng.*, 302 (2001) 37.
4. J. Gray, B. Luan, *J. Alloy. Compd.*, 336 (2002) 88.
5. X. H. Tu, L. Chen, J. F. Shen, *Int. J. Electrochem. sci.*, 7 (2012) 9573.
6. X. H. Guo, M. Zh. An, P. X. Yang, *Chinese J. Inorg. Chem.*, 25 (2009) 1254.
7. A. R. Shashikala, R. Umarani, S. M. Mayanna, *Int. J. Electrochem. sci.*, 3 (2008) 993.
8. Y. J. Zhang, C. W. Yan, F. H. Wang, H. Y. Lou, C. N. Cao, *Alloy Surf. Coat. Technol.*, 161 (2002) 36.
9. J. F. Zhang, C. W. Yan, F. H. Wang, *Appl. Surf. Sci.*, 255 (2009) 4926.
10. H. P. Liu, S. F. Bi, L. X. Cao, *Int. J. Electrochem. sci.*, 7 (2012) 8337.
11. A. L. Yerokhin, X. Nie, A. Leyland, A. Matthews, S. J. Dowey, *Surf. Coat. Technol.*, 122 (1999) 73.
12. H. F. Guo, M. Z. An, *Thin Solid Films*, 500 (2006) 186.
13. Y. G. Ko, S. Nnmgung, D. H. Shin, *Surf. Coat. Tech.*, 205 (2010) 2525.
14. F. Liu, D. Y. Shan, Y. W. Song, E. H. Han, *Surf. Coat. Tech.*, 206 (2011) 455.
15. R. F. Zhang, S. F. Zhang, Y. L. Shen, L.H. Zhang, T.Z. Liu, Y.Q. Zhang, S.B. Guo, *Appl. Surf. Sci.*, 258 (2012) 6602.
16. S. J. Xia, R. Yue, J. R. G. Rateick, V. I. Birss, *J. Electrochem. Soc.*, 151 (2004) B179.
17. X. M. Wang, L. Zhu, W. P. Li, H. C. Liu, Y. H. Li, *Appl. Sur. Sci.*, 255 (2009) 5721.
18. C. Blawert, W. Dietzel, E. Ghali, G. L. Song, *Adv. Eng. Mater.*, 8 (2006) 511.
19. O. Khaselev, D. Weiss, J. Yahalom, *J. Electrochem. Soc.*, 146 (1999) 1757.
20. S. Verdier, M. Boinet, S. Maximovitch, F. Dalard, *Corrosion Science*, 47 (2005) 1429.
21. J.R. Macdonald, Impedance Spectroscopy—Emphasizing Solid Materials and Systems, *John Wiley and Sons Inc.*, New York, 1987.
22. H. P. Duan, K. Q. Du, C. W. Yan, F. H. Wang, *Electrochimica Acta*, 51 (2006) 2898.